JMEPEG (2011) 20:198–202
DOI: 10.1007/s11665-010-9668-3

1059-9495/$19.00

Casting-Based Production of Al-TiC-AlB_2 Composite Material Through the Use of KBF_4 Salt

A.E. Karantzalis, A. Lekatou, M. Georgatis, V. Poulas, and H. Mavros

(Submitted January 7, 2010; in revised form March 16, 2010)

High volume fraction TiC-AlB_2 reinforced Al composite material has been produced by a casting process based on the use of KBF_4 salt. The reaction between the salt compound led to the release of AlB_2 precipitates in commercial purity Al melt whereas the improved wettability between the TiC particles and the formed slag caused their spontaneous entry. The resulting double reinforced composite showed no sign of severe TiC dissolution-reaction.

Keywords Al-matrix composites, halide salts, melt inoculation, TiC reinforcement

1. Introduction

Halide salts have been extensively used for more than two decades on the production of Al grain refining master alloys. A variety of commercial Al-Ti-B grain refiners are available and are generally produced by adding a mixture of KBF_4 and K_2TiF_6 salts to molten Al above 700 °C (Ref 1-3). The composition, preparation conditions, and resulting phases in relation to the final grain refining effect, have been the object of numerous experimental works and research efforts (Ref 4-10). Practically, as summarized by Mahallaway et al. (Ref 11), this inoculation process involves the reaction of the mixture of the halide salts with molten Al and the formation of Al_3Ti, TiB_2 particles, and a K-Al-F-based slag, given in simplicity by the equation:

$$2KBF_{4(s)} + 3K_2TiF_{6(s)} + 12Al_{(l)} \rightarrow 2Al_3Ti_{(s)} + TiB_{2(s)} + 5KAlF_{4(l)} + K_3AlF_{6(l)}. \quad \text{(Eq 1)}$$

The resulting first two precipitates are responsible for the grain refining phenomena and the last two liquid compounds consist the floating on the melt slag. It should be noticed that this equation refers to the production of a standard Al-5Ti-B grain refining master alloy.

One of the major problems during the production of cast Al matrix particulate composite materials is the presence of an oxide layer on the melt surface that inhibits the two phases (melt-ceramic) to get into real contact and to express their real wetting characteristics. The use of halide salts process can be a solution for these problems. The resulting from the halide process slag, with its composition, experiences a great affinity for oxide phases (Ref 12, 13). This affinity leads to the dissolution of the oxide phase, allowing the involved phases to express their real wetting characteristics, which, in the case of Al and TiC are very intensive. Under these circumstances, the particle entry into the melt can be very favorable (Ref 14-18).

The scope of the present experimental effort is to exploit the advantages of the halide salt characteristics in two ways: (a) by using KBF_4 it is possible through its reaction with molten Al to release AlB_2 precipitates within the melt and (b) by the "cleaning of oxides" character of the formed, after the reaction, slag, TiC favorable entry within the Al melt would be ensured, leading to strong and clean particle-melt interfaces. The final result is the manufacturing of a high volume fraction double-based reinforcing particle composite material. Such a composite can be used for the production of various composite materials of different Al-based matrices and reinforcement content by a diluting approach (currently under investigation). The combination of two reinforcing phases of different size can lead to improved abrasion wear performance.

2. Experimental Procedure

Commercial purity Al (CP Al, 99.7% purity, 500 g) were melt in an Salamander crucible, in a resistance heating furnace at nominal temperature of 800 °C. In order to investigate the potential of the melt-salt reaction to release boride precipitates within the melt, adequate amount of KBF_4 salt (80-100 g) was only added on the melt surface. For the production of the composite material, equal mass amounts (180 g corresponding to, approximately, 17 vol.%) of TiC powder (−325 mesh, <44 μm) and KBF_4 were mixed, spread on the melt surface and allowed to react. The equal, to the reinforcement, amount of salts was selected in order to ensure the formation of the adequate slag for both the TiC particles transfer and the release of considerable amount of boride precipitates in the melt. Prior to casting, the slag was removed and slight stirring was performed in order to homogenize the carbide and boride particles distribution. The melt was removed from the furnace and allowed to solidify within the crucible so that some particle sedimentation occurred. The overall process from the powders additions to the removal of the furnace did not exceed 5 min

A.E. Karantzalis, A. Lekatou, M. Georgatis, V. Poulas, and **H. Mavros**, Department of Materials Science and Engineering, University of Ioannina, University Campus, 45110 Ioannina, Hellas, Greece. Contact e-mail: alekatou@cc.uoi.gr

and the solidification time in the crucible was roughly 1-2 min. Specimens were received from the bottom area of the crucible and examined by means of metallography and SEM-EDX analysis. SEM inspection was carried out using a Zeiss Supra 35VP SEM equipped with a Roentec Quantax (Bruker AXs) EDS system. Particle content measurements were conducted by the aid of the 'Image J' image analysis software. XRD analysis was carried out using the Bruker D8 advance x-ray diffractometer with a Cu-Kα lamp.

3. Results and Discussion

3.1 Effect of KBF_4 Addition

Figure 1 presents the XRD spectrum of the sample where only the addition of KBF_4 salt took place. Al and AlB_2 are the two main phases that can be distinguished.

Figure 2 shows the microstructure of the solidified material region, close to the melt-slag interfacial area. Clearly, extensive formation of precipitates is observed. What is also important to mention is the characteristic string-like morphology the precipitates are associated, which is also a possible indication on the sequence of their formation during the melt-salt reactions. Similar morphologies of boride precipitates development have also been reported in the works of Fjellstedt and Jarfors (Ref 4), Feng and Froyen (Ref 19), and Mahallaway et al. (Ref 11). In the absence of any Ti carrying substances, it is reasonable to assume that the released precipitates are Al boride phases.

Figure 3 shows the distribution of boride particles at higher magnification. Clearly, gray-colored precipitates can be observed. The precipitates distribution consists of both isolated and clustered particles and their morphology varies from rod-like to plate-like shapes. Similar precipitates morphologies have been presented in other experimental efforts (Ref 4, 19). Closer examination of the boride particles shows the existence of dark spots within the bulk boride phases. Such existence is also reported in the work of Wang (Ref 20). In this research effort the dark spots have been recognized as AlB_{12} phase whereas the rest of bulk precipitate is of AlB_2 stoichiometry.

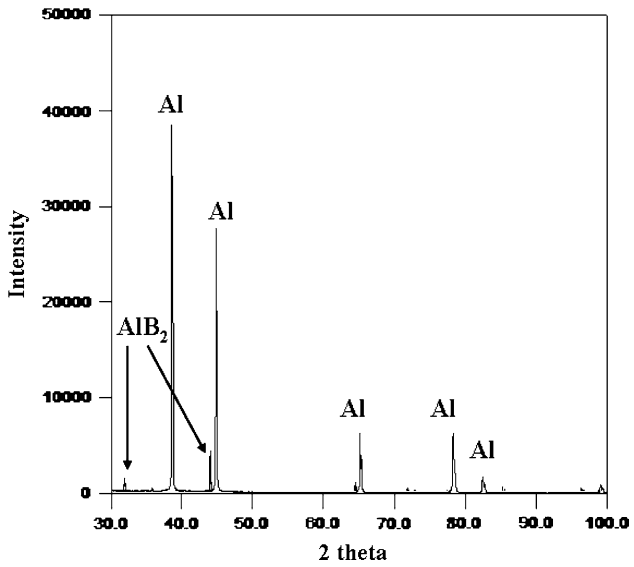

Fig. 1 XRD spectrum showing the presence of AlB_2 particles

A thermodynamic analysis is thus helpful to understand the two different boride phases presence.

According to Wang (Ref 20) there are two possible reactions that take place between KBF_4 and liquid Al:

$$12KBF_{4(s)} + 13Al_{(l)} \rightarrow AlB_{12(s)} + 12KAlF_{4(l)} \quad \text{(Eq 2)}$$

$$2KBF_{4(s)} + 3Al_{(l)} \rightarrow AlB_2 + 2KAlF_{4(l)} \quad \text{(Eq 3)}$$

Based on the same research effort (Ref 20), the free energy changes for these reactions for one mol of KBF_4 are:

$$\Delta G_{(1)} = -214.6\,\text{kJ/mol} + 9T\,\text{J/mol} \quad \text{(Eq 4)}$$

$$\Delta G_{(2)} = -267.9\,\text{kJ/mol} + 16.45\,\text{J/mol} \quad \text{(Eq 5)}$$

For the processing temperature adopted in the present effort (i.e., 820 °C = 1093 K), Eq 4 and 5 yield $\Delta G_{(1)} = -204.8$ kJ/mol and $\Delta G_{(2)} = -249.9$ kJ/mol, respectively. These values indicate that among the different boride phases, AlB_2 is the

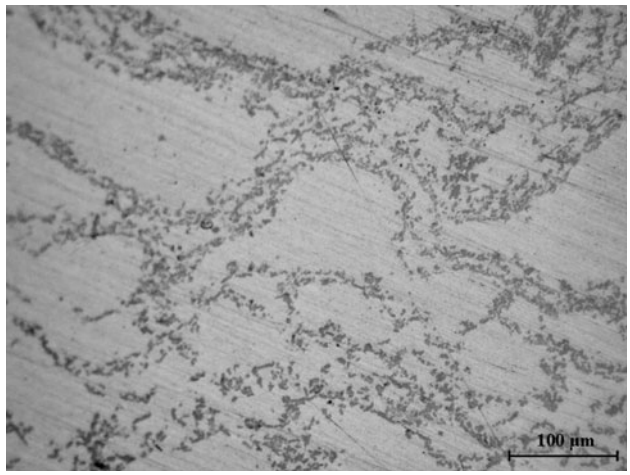

Fig. 2 Optical micrograph showing the formation of boride phases close to the melt-slag interfacial area. A characteristic string-/chain-like morphology of the boride phase development is observed

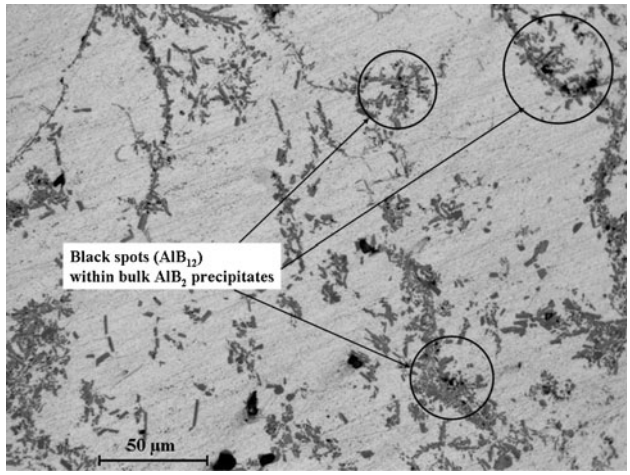

Fig. 3 Optical micrograph showing the boride phases at higher magnification. The presence of black spots (AlB_{12}) within the bulk gray boride phase (AlB_2) is observed

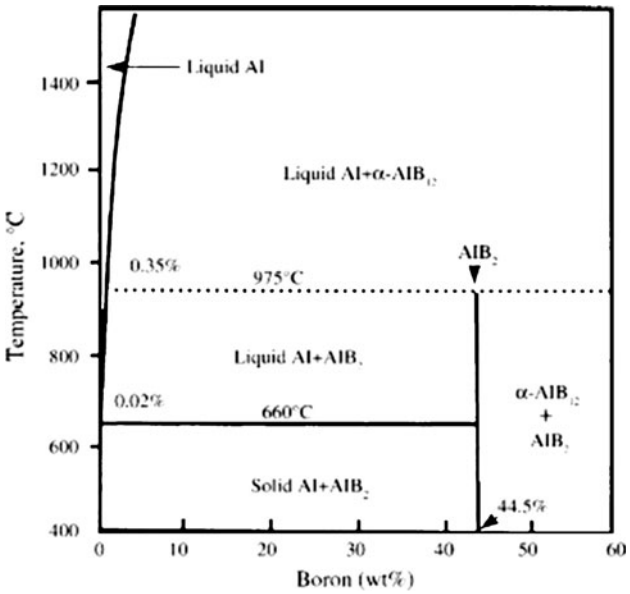

Fig. 4 The Al-B binary phase diagram (after Ref 20)

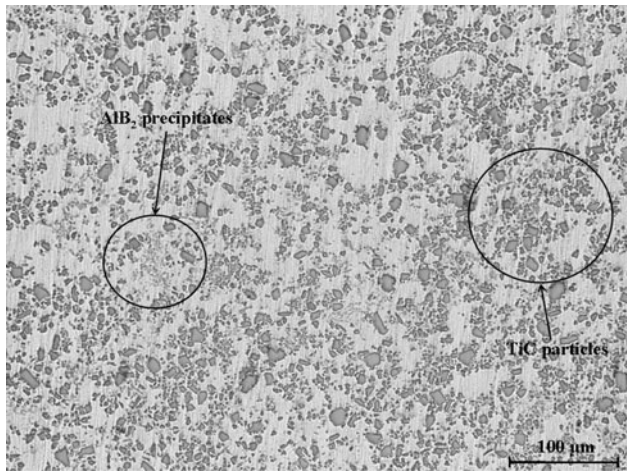

Fig. 5 Optical micrograph of the composite structure. High volume fraction of TiC particles of different size can be observed. Fine size AlB_2 particles of some clustering are also distinguished. No reaction products can be observed

most stable one and the presence of AlB_{12} should not be expected, at least at the present processing temperature. The calculated values (and consequently the phase to be expected to form) are also in agreement with the prediction of the Al-B binary phase diagram (Fig. 4). According to this, for B concentrations below 44.5 wt.%, AlB_{12} is expected to form above 975 °C and decompose to molten Al and AlB_2 through a peritectic reaction during cooling below this point. It is very interesting, hence, to explain the presence of AlB_{12} phase. There are two possible reasons for its existence:

(a) according to Murty et al. (Ref 21) the reaction between KBF_4 and molten Al is highly exothermic which means that close the slag-melt interface the temperature is risen significantly high, approaching the levels for AlB_{12} formation.
(b) the formation of a $KAlF_4$ flux layer and the low diffusion rate of B within molten Al, as reported by Prasad et al. (Ref 22), leads to a building up of B concentration close to the flux-melt interfaces, at high levels (above 44.5 wt.%) where AlB_{12} is stable according to the phase diagram. The formation of the string-like boride morphologies observed in Fig. 1, could actually be an indication of such B concentration local increase.

Despite the fact, however, that these two observations can explain the formation of AlB_{12}, they do not explain its existence at lower temperature. Wang (Ref 20) though, attributed the preservation of AlB_{12} phase to kinetic reasons such as the slow decomposition rate of AlB_{12} during the peritectic reaction.

3.2 Effect of KBF4 and TiC Simultaneous Addition

Figure 5 shows the microstructure of the resulting composite material from the bottom area of the mold. High volume fraction of TiC particles can be observed as a result of their partial sedimentation. Their size varies from medium to fine and their shape is of angular-blocky type. Their distribution can be considered as quite homogeneous, without excluding the presence of some clustering. These clusters are due to the lack of intensive stirring and the increase of the melt viscosity because of the presence of high volume fraction of ceramic particle (Ref 23). Both these reasons are making the Al melt incapable to immerse between and break up the agglomerates of the precursor powder material. Extensive mechanical stirring is a common practice in the production of cast-based Al matrix composites and its main function is to develop such a level of shear forces so that the particles are entrapped in the molten alloy. In the present effort no such extensive mechanical stirring was adopted. The basic mechanism for incorporation in the present effort was based on thermodynamic-wetting characteristics of the involved phases, in an effort to ascertain the potential of the KBF_4 salt to accomplish such a task. Hence, any other incorporation mechanism, such as mechanical stirring, would jeopardize the halide salts process incorporation capabilities.

Fine sized AlB_2 precipitates distributed within the composite, are also observed, showing, however, a more locally intensive particle clustering. Their clustering can be a result of both the lack of rigorous stirring and the increase of the melt viscosity. Their size is finer than that of the TiC particles and their shape varies from blocky-equiaxed grains to more elongated morphologies. Their formation can be explained by the statements presented in the previous paragraph. It should be noticed that the formation and growth of the AlB_2 precipitates are not associated with the presence of the TiC particles which suggests that the later did not function as possible for the AlB_2 nucleation site.

Figure 6 shows the microstructure of the composite material under SEM examination at back-scattered (BSC) mode. Clearly, the distribution of the TiC particles (white particles) is quite homogeneous with the finer particles to form limited range clustering. On the other hand, the AlB_2 precipitates (dark phases) tend to form clusters. It is also difficult in some cases to recognize them due to their compositional similarities with the matrix material. Morphologically, the AlB_2 precipitates are in agreement with the works of Wang (Ref 20), Murty et al. (Ref 21), and Mahallaway et al. (Ref 11). Image analysis

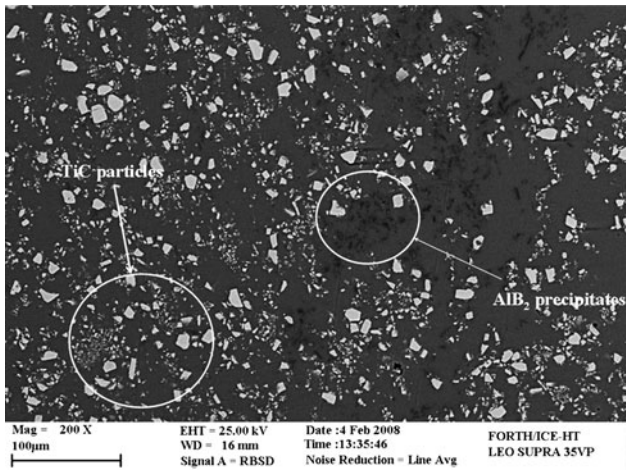

Fig. 6 Back scattered mode of SEM examination the final composite. TiC and AlB_2 particles are observed

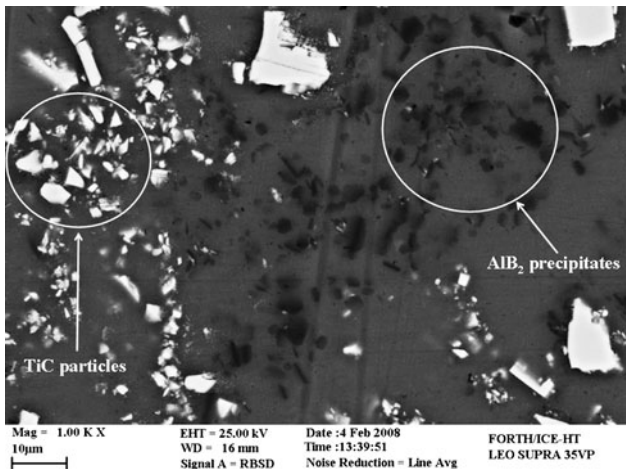

Fig. 7 SEM-BSC examination under higher magnification. No reaction-dissolution of the TiC particles products can be observed

revealed that the presence of AlB_2 precipitates varies between 6 and 8 vol.%.

Figure 7 shows a higher magnification of the microstructure under BSC mode. It is very important to mention that no reaction products at the vicinity of the TiC particles can be observed at least for this level of magnification. This suggests that the reactivity between TiC and Al is limited or, in other words, TiC exhibits sufficient stability, at least at these specific conditions. It is, however, important to concentrate further on the concept of the TiC stability under the adopted conditions.

The most common reaction to approach the reactivity between molten Al and TiC, is described by Eq 6:

$$13Al_{(l)} + 3TiC_{(s)} \rightarrow 3Al_3Ti_{(s)} + Al_4C_{3(s)} \quad \text{(Eq 6)}$$

This equation, along with the Al-rich corner of the Al-Ti-C ternary phase diagram, has been the subject of significant experimental efforts (Ref 24-27) aiming to estimate the formation and stability of the involved phases. Contreras et al. (Ref 28, 29) have calculated the free energy of equation 6and found values as follows: $\Delta G = -2.14$ kJ at 750 °C, $\Delta G = +9.71$ kJ at 800 °C, and $\Delta G = +33.62$ kJ at 900 °C per mol Al_4C_3, respectively. These calculations suggest that the reaction described by Eq 6 is thermodynamically favorable roughly below 750 °C. Such observations, in turn, permit the assumption that at higher (over 750 °C) temperatures (including the adopted processing temperature, i.e., 820 °C), Al_4C_3 and Al_3Ti are not thermodynamically stable and they can only be formed only during cooling.

These observations, explain the lack of extensive reactivity shown in Fig. 6. It is reasonable, thus, to postulate that Al_4C_3 and Al_3Ti phases are possible to form during cooling, but at limited extension, not traceable at this level of magnification, because of the short overall processing and cooling time. Prolonged processing times can lead to severe reactivity as observed elsewhere (Ref 28-30).

4. Conclusions

- Al-TiC-AlB_2 composite material was successfully fabricated through the use of a cast-based process adopting KBF_4 salt as both B provider and wetting agent.
- The reaction of KBF_4 with liquid Al lead to the formation of fine AlB_2 precipitates within the melt as well as to the formation of a $KAlF_4$-based slag that dissolves the surface oxide layer and makes the insertion of the TiC particles favorable.
- No significant sign of TiC reactivity with aluminum was observed.
- Particle sedimentation can lead to high volume fraction of the TiC phase, at the bottom area of the crucible.
- AlB_2 precipitation and TiC stability was explained by thermodynamic approaches.

Acknowledgments

The authors would like to acknowledge Dr. Vassilios Drakopoulos, Principal Scientist of the Institute of Chemical Engineering and High Temperature Process of the Foundation of Research—Greece (ICEHT/FORTH) for his assistance in the SEM examination.

References

1. D.K. Young, W.C. Setzer, F.P. Koch, R.A. Rapp, M.J. Pryor, and N. Jarrett, "Aluminum Base Alloy and Method for Preparing Same," US Patent, 5,415,708, 1995
2. L. Backerund, R. Kiusalaas, H. Klang, M. Vader, J. Noordegraaf, and E.H.K. Nagelvoort, "Method for Production of Master Alloys for Grain Refining Treatment of Aluminum Melts," US Patent, 5,104,616, 1992
3. P. Davies, J.L.F. Kellie, D.P. Patron, and J.V. Wood, "Metal Matrix Alloys," US Patent, 6,228,185, 2001
4. J. Fjellstedt and A.E.W. Jarforfs, On the Precipitation of TiB_2 in Aluminum Melts from the Reaction with KBF_4 and K_2TiF_6, *Mater. Sci. Eng. A*, 2005, **413-414**, p 527–532
5. J. Fjellstedt, A.E.W. Jarforfs, and L. Svedsen, Experimental Analysis of the Intermediary Phases AlB_2, AlB_{12} and TiB_2 in the Al-B and Al-Ti-B Systems, *J. Alloys Comp.*, 1999, **283**, p 192–197
6. Y. Birol, An Improved Practice to Manufacture Al-Ti-B Master Alloys by Reacting Halide Salts with Molten Aluminium, *J. Alloys Comp.*, 2006, **420**, p 71–76

7. Y. Birol, Effect of the Salt Addition Practice on the Grain Refining Efficiency of Al-Ti-B Master Alloys, *J. Alloys Comp.*, 2006, **420**, p 207–212
8. Y. Birol, The Effect of Holding Conditions in the Conventional Halide Salt Procession the Performance of Al-Ti-B Grain Refiner Alloys, *J. Alloys Comp.*, 2007, **427**, p 142–147
9. Y. Birol, Production of Al-Ti-B Grain Refining Master Alloys from B_2O_3 and K_2TiF_6, *J. Alloys Comp.*, 2007, **443**, p 94–98
10. Y. Birol, Production of Al-Ti-B Master Alloys from Ti Sponge and KBF_4, *J. Alloys Comp.*, 2007, **440**, p 108–112
11. N.E. Mahallaway, M.A. Taha, A.E.W. Jarfors, and H. Fredriksson, On the Reaction Between Aluminium, K_2TiF_6 and KBF_4, *J. Alloys Comp.*, 1992, **292**, p 221–229
12. S. Boghosian, A.A. Goda, H. Mediaas, W. Ravlo, and T. Østvold, Oxide Complexes in Alkali-Alkaline-Earth Chloride Melts, *Acta Chem. Scan. Ser.*, 1991, **A45**, p 145–157
13. H. Mediaas, J.F. Vindstad, and T. Østvold, Solubility of MgO in Mixed Chloride-Fluoride Melts Containing $MgCl_2$, *Acta Chem. Scan. Ser.*, 1997, **A51**, p 504–514
14. A.R. Kennedy, A.E. Karantzalis, J.V. Wood, J.D. Ellis, and J.L.F. Kellie, "Metal Matrix Composites," UK Patent, GB 2316092A, 1998
15. A.R. Kennedy and A.E. Karantzalis, The Incorporation of Ceramic Particles into Molten Aluminium and the Relationship to Contact Angle Data, *Mater. Sci. Eng.*, 1999, **A264**, p 122–129
16. A.R. Kennedy, A.E. Karantzalis, and S.M. Wyatt, The Microstructure and the Mechanical Properties of TiC and TiB_2 Reinforced Cast Metal Matrix Composites, *J. Mater. Sci.*, 1999, **34**, p 933–940
17. A.R. Kennedy and A.E. Karantzalis, The Grain Refining Action of TiB_2 and TiC Particles Added to Al by a Stir-Casting Method, *Mater. Sci. Forum*, 1996, **217–222**, p 253–258
18. A.E. Karantzalis, S.M. Wyatt, and A.R. Kennedy, The Mechanical Properties of Al-TiC Metal Matrix Composites Fabricated by a Stir-Casting Technique, *Mater. Sci. Eng.*, 1997, **A237**, p 200–206
19. C.F. Feng and L. Froyen, Microstructures of In Situ Al/TiB_2 MMCs Prepared by a Casting Route, *J. Mater. Sci.*, 2000, **35**, p 837–850
20. X. Wang, The Formation of AlB_2 in an Al-B Master Alloy, *J. Alloys Comp.*, 2005, **403**, p 283–287
21. B.S. Murty, S.A. Kori, K. Venkateswarlu, R.R. Bhat, and M. Chakraborty, Manufacture of Al-Ti-B Master Alloys by the Reaction of Complex Halide Salts with Molten Aluminium, *J. Mater. Proces. Techn.*, 1999, **89–90**, p 152–158
22. K.V.S. Prasad, B.S. Murty, P. Pramanik, P.G. Mukunda, and M. Chakraborty, Reaction of Fluoride Salts with Aluminium, *Mater. Sci. Technol.*, 1996, **12**, p 766–770
23. K.R. Ravi, R.M. Pillai, K.R. Amaranathan, B.C. Pai, and M. Chakrabotry, Fluidity of Aluminum Alloys and Composites: A Review, *J. Alloys Comp.*, 2008, **456**(1-2), p 201–210
24. L. Svendsen and A. Jarfors, Al-Ti-C Phase Diagram, *Mater. Sci. Technol.*, 1993, **9**(11), p 948–957
25. A. Jarfors, H. Fredriksson, and L. Froyen, On the Thermodynamics and Kinetics of Carbides in the Aluminium-rich Corner of the Al-Ti-C Phase Diagram, *Mater. Sci. Eng.*, 1991, **A135**, p 119–123
26. J.C. Viala, N. Peillon, L. Clochefert, and J. Bouix, Diffusion Paths and Reaction Mechanisms in the High Temperature Chemical Interaction Between Carbon and Titanium Aluminides, *Mater. Sci. Eng.*, 1995, **A203**, p 222–237
27. H. Ding, X. Liu, L. Yua, and G. Zhao, The Influence of Forming Processes on the Distribution and Morphologies of TiC in Al-Ti-C Master Alloys, *Scr. Mater.*, 2007, **57**, p 575–578
28. A. Contreras, C. Angeles-Chávez, O. Flores, and R. Perez, Structural, Morphological and Interfacial Characterization of Al-Mg/TiC Composites, *Mater. Character.*, 2007, **58**, p 685–693
29. A. Contreras, E. Bedolla, and R. Perez, Interfacial Phenomena in Wettability of TiC by Al-Mg Alloys, *Acta Mater.*, 2004, **52**, p 985–994
30. V.H. Lopez, A. Scoles, and A.R. Kennedy, The Thermal Stability of TiC Particles in an Al7wt.%Si Alloy, *Mater. Sci. Eng.*, 2003, **A356**, p 316–325